

VGS-Decoding: Visual Grounding Score Guided Decoding for Hallucination Mitigation in Medical VLMs

Govinda Kolli^{1,2}, Adinath Madhavrao Dukre¹, Behzad Bozorgtabar³,
Dwarikanath Mahapatra⁴, Imran Razzak¹

¹MBZUAI, Abu Dhabi, UAE

²Rajiv Gandhi University of Knowledge Technologies, India

³Aarhus University, Aarhus, Denmark

⁴Khalifa University, Abu Dhabi, UAE

Abstract. Medical Vision-Language Models (VLMs) often hallucinate by generating responses based on language priors rather than visual evidence, posing risks in clinical applications. We propose Visual Grounding Score Guided Decoding (VGS-Decoding), a training-free method to mitigate hallucinations during inference. Our key insight is that hallucinated tokens maintain or increase their probability when visual information is degraded, while visually grounded tokens decrease in probability. We introduce the Visual Grounding Score (VGS), which measures each token’s visual dependency by comparing distributions from original and distorted images. During decoding, we reweight probabilities by amplifying visually grounded tokens while suppressing hallucinations. Unlike fixed-weight contrastive methods, VGS-Decoding provides per-token adaptive control. Experiments on MIMIC-Diff-VQA and VQA-RAD across LLaVA-Med, CheXagent, and MedGemma demonstrate consistent improvements, with up to +9.12% overall gain and +8.98% in open-ended recall, while introducing only 2× inference overhead and no additional training, making it practical for clinical deployment. Upon acceptance, code will be released publicly to facilitate reproducibility.

Keywords: Medical VQA · Hallucination Mitigation · Vision-Language Models · Visual Grounding · Contrastive Decoding

1 Introduction

Medical Vision-Language Models (VLMs) have emerged as powerful tools for clinical applications, demonstrating remarkable capabilities in tasks such as visual question answering (VQA), radiology report generation, and diagnostic assistance [3,16,24]. Models like LLaVA-Med [16], trained on large-scale biomedical image-text pairs, have shown promising performance on medical VQA benchmarks including VQA-RAD [14] and MIMIC-Diff-VQA [11]. Despite these advances, medical VLMs remain vulnerable to hallucinations, generating clinically plausible but factually incorrect responses that are unsupported by the visual

evidence [9, 25]. In high-stakes medical scenarios, such hallucinations pose significant risks, potentially leading to misdiagnosis and inappropriate clinical decisions, and dangerous automation bias [26].

Hallucinations in VLMs primarily arise from over-reliance on language priors rather than visual information [8, 12, 15], where models draw upon statistical patterns learned during training. This is particularly problematic in medical VQA, where precise identification of anatomical locations, pathological findings, and diagnostic details is critical. Several decoding-time strategies have been proposed to mitigate hallucinations in general-domain VLMs, building upon foundational contrastive decoding techniques in NLP [17]. Visual Contrastive Decoding (VCD) [15] contrasts output distributions from original and noise-distorted images using a subtractive formula in log-space. Decoding by Contrasting Layers(DoLA) [4] exploits the hierarchical encoding of factual knowledge in transformer layers by contrasting early and late layer outputs. Over-trust Penalty and a Retrospection-Allocation(OPERA) [12] introduces a penalty term during beam search to address over-trust in summary tokens. While these methods have shown effectiveness on general VQA benchmarks like POPE [18] and MME [7], we find that they often fail on medical VQA, sometimes degrading performance by over 6% compared to baseline greedy decoding. This failure stems from the unique characteristics of medical VQA: shorter responses, specialized vocabulary, and the critical importance of precise anatomical and pathological terms where aggressive correction can be harmful.

In this paper, we propose Visual Grounding Score Guided Decoding (VGS-Decoding), a training-free method specifically designed for hallucination mitigation in medical VQA. Our key insight is that hallucinated tokens exhibit a distinctive signature: when visual information is degraded, hallucinated tokens maintain or *increase* their probability (being driven by language priors), while visually grounded tokens *decrease* in probability. We formalize this observation through the Visual Grounding Score (VGS), a novel metric that quantifies each token’s visual dependency. Unlike VCD’s fixed-weight subtractive approach, VGS provides a bounded, interpretable measure in $[-1, +1]$ that enables *per-token adaptive* correction through multiplicative reweighting.

This formulation offers several advantages: (1) tokens with high VGS (visually grounded) are amplified, (2) tokens with negative VGS (potential hallucinations) are suppressed, and (3) neutral tokens remain largely unchanged, preserving the model’s linguistic coherence.

We evaluate VGS-Decoding on two medical VQA benchmarks (VQA-RAD [14] and MIMIC-Diff-VQA [11]) across three diverse medical VLMs (LLaVA-Med, CheXagent [3], and MedGemma [24]). Our experiments reveal that VGS-Decoding is the only method that consistently improves all models, achieving up to +9.12% overall improvement. In contrast, existing methods (VCD, DoLA, OPERA) frequently degrade performance on medical VQA, highlighting the need for domain-specific solutions. Our main contributions are:

- We identify that existing hallucination mitigation methods often fail on medical VQA, motivating the need for domain-adapted approaches.

- We propose the Visual Grounding Score (VGS), a novel metric that quantifies token-level visual dependency through normalized probability difference.
- We introduce VGS-Decoding, a training-free method that achieves consistent improvements across diverse medical VLMs and datasets.

2 Method

We present Visual Grounding Score Guided Decoding (VGS-Decoding), a training-free approach for mitigating hallucinations in medical VLMs. Our method operates during inference by adaptively reweighting token probabilities based on their visual grounding score. Fig 1 illustrates the overall framework.

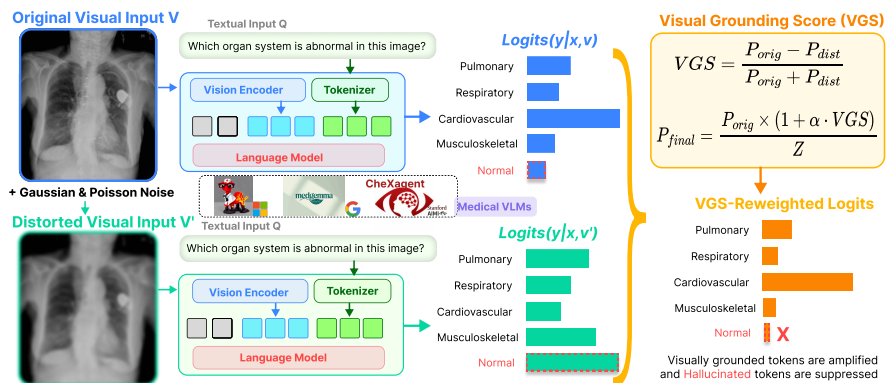


Fig. 1. Overview of VGS-Decoding. Both the original image V and its noise-distorted version V' are passed through the medical VLM, producing token distributions P_{orig} (blue) and P_{dist} (green). The Visual Grounding Score (VGS) is computed as their normalized probability difference and used for multiplicative reweighting: visually grounded tokens (positive VGS) are amplified, while hallucinated tokens (negative VGS, \times) are suppressed.

2.1 Preliminaries

Given a medical image V and a text query Q , a vision-language model generates a response token-by-token in an autoregressive manner. At each decoding step t , the model produces a probability distribution over the vocabulary:

$$P_{orig}(y_t|V, Q, y_{<t}) = \text{softmax}(z_t) \quad (1)$$

where z_t denotes the logits and $y_{<t}$ represents previously generated tokens. Standard greedy decoding selects $y_t = \arg \max_y P_{orig}(y)$.

Hallucinations occur when the model generates tokens based on language priors rather than visual evidence [6, 23]. For instance, when asked about the

location of a finding in a chest X-ray, a model might generate “left” based on statistical co-occurrence patterns even when the image shows a right-sided abnormality.

2.2 Visual Grounding Score

Our method is motivated by a key observation: visually grounded tokens and hallucinated tokens exhibit distinct behaviors when visual information is degraded. Specifically, visually grounded tokens show decreased probability when the image is corrupted, as the model loses access to the supporting visual evidence. In contrast, hallucinated tokens maintain or even increase their probability under visual corruption, since these tokens are driven by language priors rather than actual visual content.

To exploit this behavioral signature, we first construct a distorted version of the input image $V' = \mathcal{D}(V)$ by applying a combination of Gaussian and Poisson noise [2, 10, 19]:

$$V' = V + \mathcal{N}(0, \sigma^2) + \text{Poisson}(\lambda) \quad (2)$$

where σ and λ control the noise intensity. We then obtain the probability distribution conditioned on the distorted image:

$$P_{\text{dist}}(y_t | V', Q, y_{<t}) = \text{softmax}(\mathbf{z}'_t) \quad (3)$$

We define the Visual Grounding Score (VGS) as the normalized difference between the original and distorted distributions:

$$\text{VGS}(t) = \frac{P_{\text{orig}}(t) - P_{\text{dist}}(t)}{P_{\text{orig}}(t) + P_{\text{dist}}(t)} \quad (4)$$

The VGS metric offers several desirable properties. First, it is bounded within $[-1, +1]$, ensuring stable and interpretable values throughout the decoding process. A positive VGS indicates that the token is visually grounded, as its probability decreases when visual information is degraded. Conversely, a negative VGS suggests potential hallucination, where the token’s probability increases or remains stable without proper visual support. A VGS near zero indicates visual independence, typical of function words that are equally likely regardless of image quality.

2.3 VGS-Guided Decoding

Using the VGS metric, we reweight the original probability distribution to amplify visually grounded tokens while suppressing potential hallucinations:

$$P_{\text{final}}(t) \propto P_{\text{orig}}(t) \times \max(1 + \alpha \cdot \text{VGS}(t), \delta) \quad (5)$$

where $\alpha > 0$ controls the reweighting strength and $\delta > 0$ is a small constant (default $\delta = 0.01$) to prevent zero probabilities. The final distribution is normalized to sum to one.

Algorithm 1 VGS-Decoding

Require: Image V , query Q , model \mathcal{M} , strength α , noise params (σ, λ) **Ensure:** Generated response Y

- 1: $V' \leftarrow V + \mathcal{N}(0, \sigma^2) + \text{Poisson}(\lambda)$
- 2: $Y \leftarrow []$
- 3: **while** not end-of-sequence **do**
- 4: $P_{\text{orig}} \leftarrow \mathcal{M}(V, Q, Y)$
- 5: $P_{\text{dist}} \leftarrow \mathcal{M}(V', Q, Y)$
- 6: **for** each token t in vocabulary **do**
- 7: $\text{VGS}(t) \leftarrow \frac{P_{\text{orig}}(t) - P_{\text{dist}}(t)}{P_{\text{orig}}(t) + P_{\text{dist}}(t)}$
- 8: $P_{\text{final}}(t) \leftarrow P_{\text{orig}}(t) \times \max(1 + \alpha \cdot \text{VGS}(t), \delta)$
- 9: **end for**
- 10: $P_{\text{final}} \leftarrow P_{\text{final}} / \sum P_{\text{final}}$
- 11: $y \leftarrow \arg \max P_{\text{final}}$
- 12: $Y \leftarrow Y \cup \{y\}$
- 13: **end while**
- 14: **return** Y

The multiplicative factor $(1 + \alpha \cdot \text{VGS}(t))$ provides adaptive correction based on each token’s visual grounding. When $\text{VGS}(t) > 0$, the factor exceeds one, amplifying visually grounded tokens. When $\text{VGS}(t) < 0$, the factor falls below one, suppressing potentially hallucinated tokens. When $\text{VGS}(t) \approx 0$, the factor remains close to one, preserving neutral tokens such as function words. This per-token adaptive mechanism ensures that correction strength is proportional to the degree of visual grounding or hallucination.

2.4 Algorithm

Algorithm 1 summarizes the complete VGS-Decoding procedure. The image is distorted once before decoding begins. At each decoding step, we compute probability distributions from both the original and distorted images, calculate the VGS for each vocabulary token, apply the multiplicative reweighting, and select the token with maximum adjusted probability.

2.5 Computational Complexity

VGS-Decoding requires two forward passes per decoding step, one for the original image and one for the distorted image, resulting in approximately twice the inference time of standard greedy decoding. This computational cost is comparable to VCD and significantly lower than OPERA, which requires beam search with multiple candidates. The image distortion is performed once before decoding begins and adds negligible overhead.

3 Experiments

3.1 Datasets

We evaluate VGS-Decoding on two medical VQA benchmarks. VQA-RAD [14] contains 315 radiology images including CT, MRI, and X-ray with 3,515 question-answer pairs. Following standard practice, we use the test set comprising 451 questions with 200 open-ended and 251 closed-ended samples, covering diverse clinical queries about anatomical structures, abnormalities, and imaging modalities. MIMIC-Diff-VQA [11] is derived from the MIMIC-CXR database [13] and focuses on longitudinal chest X-ray analysis with question-answer pairs about differences between sequential radiographs. We evaluate on 13,121 test samples with 8,380 open-ended and 4,741 closed-ended questions to assess generalization to larger-scale medical VQA.

3.2 Models

We evaluate three diverse medical VLMs to demonstrate generalizability. LLaVA-Med [16] is a 7B parameter model adapted from LLaVA through curriculum learning on biomedical image-text pairs from PubMed Central, representing general-purpose medical VLMs. CheXagent [3] is a 3B parameter model specifically trained on MIMIC-CXR’s official training set [13] for chest X-ray interpretation, representing domain-specialized medical VLMs with strong in-domain performance. MedGemma [24] is a 4B parameter model from Google trained on diverse medical imaging data, representing efficient smaller-scale medical VLMs.

3.3 Baselines

We compare VGS-Decoding against four decoding strategies. Greedy decoding selects the highest probability token at each step, serving as the baseline without any hallucination mitigation. VCD [15] contrasts distributions from original and noise-distorted images using a subtractive log-space formula with recommended settings of $\alpha = 1.0$ and diffusion noise. DoLA [4] contrasts early and late transformer layers to surface factual knowledge using dynamic layer selection as recommended. OPERA [12] applies over-trust penalty and retrospection-allocation during beam search decoding with beam size 5, though it is computationally expensive and less effective on short-length generations typical in medical VQA [20], as beam search is known to suffer from length bias and degradation in open-ended generation tasks [22].

Evaluation Metrics. Following standard medical VQA evaluation protocols [1, 14, 16], we report three metrics. Closed-ended accuracy measures the percentage of correctly answered yes/no and multiple-choice questions, evaluating precise clinical judgment. Open-ended recall computes token-level recall between generated and ground-truth answers, measuring coverage of key medical terms. Overall accuracy provides a weighted combination based on question type distribution.

Implementation Details For VGS-Decoding, we apply Gaussian noise with

Table 1. Performance comparison on VQA-RAD (200 open + 251 closed) and MIMIC-Diff-VQA (8,380 open + 4,741 closed). Best results in **bold**. VGS-Decoding is the only method that consistently improves all models.

Model	Method	VQA-RAD				Δ	MIMIC-Diff-VQA			
		Open	Closed	Overall	Δ		Open	Closed	Overall	Δ
LLaVA-Med	Greedy	34.45	68.92	53.64	–	28.04	48.39	35.39	–	
	VCD	30.85	61.20	47.71	-5.93	25.98	46.42	33.33	-2.06	
	DoLA	32.76	58.96	47.34	-6.30	28.75	47.94	35.68	+0.29	
	OPERA	33.22	61.69	49.05	-4.59	21.18	46.02	30.14	-5.25	
	VGS (Ours)	38.90	72.91	57.75	+4.11	30.84	55.79	39.86	+4.47	
CheXagent	Greedy	22.02	70.92	49.24	–	44.06	82.07	57.79	–	
	VCD	21.73	68.53	47.78	-1.46	38.88	79.14	53.42	-4.37	
	DoLA	20.73	68.92	47.55	-1.69	39.78	81.94	55.02	-2.77	
	OPERA	20.50	69.32	47.67	-1.57	36.19	82.03	52.75	-5.04	
	VGS (Ours)	23.48	71.31	50.10	+0.86	43.99	82.53	57.91	+0.12	
MedGemma	Greedy	49.50	61.75	56.32	–	25.97	73.55	43.16	–	
	VCD	50.29	57.77	54.45	-1.87	29.38	68.76	43.61	+0.45	
	DoLA	51.91	72.51	63.38	+7.06	32.56	76.82	48.55	+5.39	
	OPERA	48.90	65.74	58.27	+1.95	28.35	75.53	45.40	+2.24	
	VGS (Ours)	53.05	73.58	64.48	+8.16	34.95	82.91	52.28	+9.12	

$\sigma = 0.07$ and Poisson noise with $\lambda = 70$ for image distortion. The reweighting strength is set to $\alpha = 1.0$ as default across all models for fair comparison. All experiments use greedy decoding. Inference is performed on NVIDIA A100 GPUs. Statistical significance is computed using McNemar’s test [21] with 10,000 bootstrap samples [5].

3.4 Results

Main Results Table 1 and Fig 2 presents the comparison across all models and datasets. VGS-Decoding achieves consistent improvements across experimental settings, improving all three models on both datasets and achieving best results on 6 out of 6 model-dataset combinations. Existing methods frequently degrade performance on medical VQA, with VCD showing up to -5.93% and OPERA up to -5.25% drops. The largest improvements are observed on MedGemma with $+8.16\%$ on VQA-RAD and $+9.12\%$ on MIMIC-Diff-VQA. For CheXagent on MIMIC-Diff-VQA, VGS-Decoding maintains baseline performance ($+0.12\%$), which is expected as CheXagent was specifically trained on MIMIC-CXR’s official training set. Notably, VGS-Decoding is the only method that does not significantly degrade this well-calibrated model’s performance, unlike VCD (-4.37%), DoLA (-2.77%), and OPERA (-5.04%).

Ablation Study Table 2 analyzes the contribution of each component in VGS-Decoding. VCD-style fixed-weight contrastive decoding degrades performance

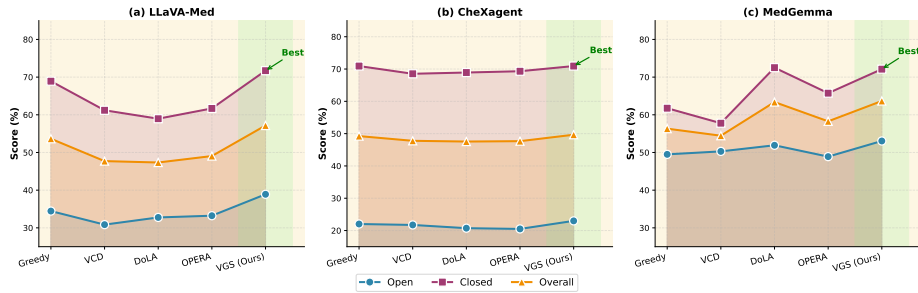


Fig. 2. Decoding method comparison on VQA-RAD. VGS-Decoding consistently outperforms baselines across all three medical VLMs.

Table 2. Component ablation study of VGS-Decoding on VQA-RAD (LLaVA-Med). Each row adds one component incrementally.

Configuration	Open	Closed	Overall	Δ
Baseline (Greedy)	34.45	68.92	53.64	–
+ Fixed weight (VCD-style)	30.85	61.20	47.71	-5.93
+ VGS metric only	35.49	69.32	54.32	+0.68
+ VGS + Mult. reweight	38.90	72.91	57.75	+4.11

Table 3. Effect of reweighting strength α on VQA-RAD. $\alpha=0.0$ corresponds to greedy decoding. Optimal values per model are in **bold**.

α	LLaVA-Med		MedGemma	
	Overall	p -value	Overall	p -value
0.0	53.64	–	56.32	–
0.5	56.95	0.046	59.00	0.002
1.0	57.75	0.025	64.48	0.001
1.5	58.79	0.001	64.37	<0.001
2.0	57.50	0.014	65.90	<0.001

by -5.93% , confirming that existing methods fail on medical VQA. Computing VGS alone without reweighting provides modest improvement of $+0.68\%$, demonstrating that the metric captures useful signal. The full VGS-Decoding with multiplicative reweighting achieves the best results with $+4.11\%$ improvement, showing that both the VGS metric and adaptive reweighting are necessary.

Table 3 examines the effect of reweighting strength α . All non-zero values achieve statistically significant improvements over baseline ($p < 0.05$). Optimal α varies by model, with 1.5 for LLaVA-Med and 2.0 for MedGemma, but $\alpha = 1.0$ provides consistent improvements across all models and is used as default.

4 Conclusion

We proposed VGS-Decoding, a training-free method that mitigates hallucinations in medical VLMs by adaptively reweighting token probabilities via the Visual Grounding Score (VGS), which exploits the observation that hallucinated tokens are resilient to visual degradation while grounded tokens are not. Experiments on VQA-RAD and MIMIC-Diff-VQA across LLaVA-Med, CheXagent, and MedGemma demonstrate that VGS-Decoding is the only method that consistently improves all models, achieving up to +9.12% overall improvement with only $2\times$ inference overhead and no additional training.

References

1. Antol, S., Agrawal, A., Lu, J., Mitchell, M., Batra, D., Zitnick, C.L., Parikh, D.: Vqa: Visual question answering. In: Proceedings of the IEEE International Conference on Computer Vision (ICCV) (December 2015)
2. Bushberg, J.T., Seibert, J.A., Leidholdt Jr, E.M., Boone, J.M.: The essential physics of medical imaging. Lippincott Williams & Wilkins (2011)
3. Chen, Z., Varma, M., Xu, J., Paschali, M., Van Veen, D., Johnston, A., Youssef, A., Blankemeier, L., Bluethgen, C., Altmayer, S., et al.: A vision-language foundation model to enhance efficiency of chest x-ray interpretation. arXiv preprint arXiv:2401.12208 (2024)
4. Chuang, Y.S., Xie, Y., Luo, H., Kim, Y., Glass, J., He, P.: Dola: Decoding by contrasting layers improves factuality in large language models. arXiv preprint arXiv:2309.03883 (2023)
5. Dror, R., Baumer, G., Shlomov, S., Reichart, R.: The hitchhiker’s guide to testing statistical significance in natural language processing. In: Gurevych, I., Miyao, Y. (eds.) Proceedings of the 56th Annual Meeting of the Association for Computational Linguistics (Volume 1: Long Papers). pp. 1383–1392. Association for Computational Linguistics, Melbourne, Australia (Jul 2018). <https://doi.org/10.18653/v1/P18-1128>, <https://aclanthology.org/P18-1128/>
6. Favero, A., Zancato, L., Trager, M., Choudhary, S., Perera, P., Achille, A., Swaminathan, A., Soatto, S.: Multi-modal hallucination control by visual information grounding. In: Proceedings of the IEEE/CVF Conference on Computer Vision and Pattern Recognition. pp. 14303–14312 (2024)
7. Fu, C., Chen, P., Shen, Y., Qin, Y., Zhang, M., Lin, X., Yang, J., Zheng, X., Li, K., Sun, X., et al.: Mme: A comprehensive evaluation benchmark for multimodal large language models. arXiv preprint arXiv:2306.13394 (2023)
8. Goyal, Y., Khot, T., Summers-Stay, D., Batra, D., Parikh, D.: Making the v in vqa matter: Elevating the role of image understanding in visual question answering. In: Proceedings of the IEEE conference on computer vision and pattern recognition. pp. 6904–6913 (2017)
9. Gu, Z., Chen, J., Liu, F., Yin, C., Zhang, P.: Medvh: Toward systematic evaluation of hallucination for large vision language models in the medical context. *Advanced Intelligent Systems* **8**(1), 2500255 (2026)
10. Hendrycks, D., Dietterich, T.: Benchmarking neural network robustness to common corruptions and perturbations. arXiv preprint arXiv:1903.12261 (2019)

11. Hu, X., Gu, L., An, Q., Zhang, M., Liu, L., Kobayashi, K., Harada, T., Summers, R.M., Zhu, Y.: Expert knowledge-aware image difference graph representation learning for difference-aware medical visual question answering. In: Proceedings of the 29th ACM SIGKDD Conference on Knowledge Discovery and Data Mining. pp. 4156–4165 (2023)
12. Huang, Q., Dong, X., Zhang, P., Wang, B., He, C., Wang, J., Lin, D., Zhang, W., Yu, N.: Opera: Alleviating hallucination in multi-modal large language models via over-trust penalty and retrospection-allocation. In: Proceedings of the IEEE/CVF Conference on Computer Vision and Pattern Recognition. pp. 13418–13427 (2024)
13. Johnson, A.E., Pollard, T.J., Greenbaum, N.R., Lungren, M.P., Deng, C.y., Peng, Y., Lu, Z., Mark, R.G., Berkowitz, S.J., Horng, S.: Mimic-cxr-jpg, a large publicly available database of labeled chest radiographs. arXiv preprint arXiv:1901.07042 (2019)
14. Lau, J.J., Gayen, S., Ben Abacha, A., Demner-Fushman, D.: A dataset of clinically generated visual questions and answers about radiology images. *Scientific data* **5**(1), 1–10 (2018)
15. Leng, S., Zhang, H., Chen, G., Li, X., Lu, S., Miao, C., Bing, L.: Mitigating object hallucinations in large vision-language models through visual contrastive decoding. In: Proceedings of the IEEE/CVF Conference on Computer Vision and Pattern Recognition (CVPR). pp. 13872–13882 (June 2024)
16. Li, C., Wong, C., Zhang, S., Usuyama, N., Liu, H., Yang, J., Naumann, T., Poon, H., Gao, J.: Llava-med: Training a large language-and-vision assistant for biomedicine in one day. *Advances in Neural Information Processing Systems* **36**, 28541–28564 (2023)
17. Li, X.L., Holtzman, A., Fried, D., Liang, P., Eisner, J., Hashimoto, T.B., Zettlemoyer, L., Lewis, M.: Contrastive decoding: Open-ended text generation as optimization. In: Proceedings of the 61st annual meeting of the association for computational linguistics (volume 1: Long papers). pp. 12286–12312 (2023)
18. Li, Y., Du, Y., Zhou, K., Wang, J., Zhao, W.X., Wen, J.R.: Evaluating object hallucination in large vision-language models. In: Proceedings of the 2023 conference on empirical methods in natural language processing. pp. 292–305 (2023)
19. Liao, Z., Hu, S., Zou, K., Fu, H., Zhen, L., Xia, Y.: Vision-Amplified Semantic Entropy for Hallucination Detection in Medical Visual Question Answering . In: proceedings of Medical Image Computing and Computer Assisted Intervention – MICCAI 2025. vol. LNCS 15964. Springer Nature Switzerland (September 2025)
20. Liu, B., Zhan, L.M., Xu, L., Ma, L., Yang, Y., Wu, X.M.: Slake: A semantically-labeled knowledge-enhanced dataset for medical visual question answering. In: 2021 IEEE 18th international symposium on biomedical imaging (ISBI). pp. 1650–1654. IEEE (2021)
21. McNemar, Q.: Note on the sampling error of the difference between correlated proportions or percentages. *Psychometrika* **12**(2), 153–157 (1947)
22. Meister, C., Cotterell, R., Vieira, T.: If beam search is the answer, what was the question? In: Proceedings of the 2020 Conference on Empirical Methods in Natural Language Processing (EMNLP). pp. 2173–2185 (2020)
23. Rohrbach, A., Hendricks, L.A., Burns, K., Darrell, T., Saenko, K.: Object hallucination in image captioning. In: Proceedings of the 2018 Conference on Empirical Methods in Natural Language Processing. pp. 4035–4045 (2018)
24. Sellergren, A., Kazemzadeh, S., Jarosensri, T., Kiraly, A., Traverse, M., Kohlberger, T., Xu, S., Jamil, F., Hughes, C., Lau, C., et al.: Medgemma technical report. arXiv preprint arXiv:2507.05201 (2025)

25. Xu, Z., Jain, S., Kankanhalli, M.: Hallucination is inevitable: An innate limitation of large language models. arXiv preprint arXiv:2401.11817 (2024)
26. Zheng, Y., Gan, W., Chen, Z., Qi, Z., Liang, Q., Yu, P.S.: Large language models for medicine: a survey. *International Journal of Machine Learning and Cybernetics* **16**(2), 1015–1040 (2025)